Journal of The Electrochemical Society, **147** (9) 3302-3310 (2000)
S0013-4651(99)04-103-8 CCC: $7.00

Some Electrochemical Studies on Cementation of Copper onto Zinc from Sulfate Bath

K. G. Mishra and R. K. Paramguru

Council of Scientific and Industrial Research, Regional Research Laboratory, Bhubaneswar-751 013, Orissa, India

Cementation of copper onto zinc from a sulfate bath was investigated through polarization measurements of both the anodic and cathodic half-cell reactions as well as practical cementation studies. Individual half-cell reactions, when isolated in a dual cell, followed a first-order rate with respect to $[Cu^{2+}]$ (cathodic) without any excess zinc dissolution (at the anode) via a hydrogen reaction. In the presence of a zinc surface and Cu^{2+} in a single bath, excess zinc dissolved via hydrogen reduction and the first-order copper cementation rate was enhanced after an initial slow step. The enhanced rate is associated with a decrease of the mixed potential, E_m. Deposited copper catalyzes, excess zinc dissolution via hydrogen reduction reaction.

Manuscript submitted April 26, 1999; revised manuscript received June 2, 2000.

Cementation of copper onto zinc dust from sulfate leach liquor is a common method of purification in zinc refineries, which follow the roast-leach-electrowining route to produce zinc. The reaction may be represented as follows

$$Zn(s) + Cu^{2+} \rightarrow Cu(s) + Zn^{2+} \quad [1]$$

This is a heterogeneous electrochemical reaction involving reduction of copper ions to zero valence at the zinc metal surface site and dissolution of zinc at another surface site of the same metal. This electrochemical phenomenon, where anodic and cathodic sites are short-circuited, proceeded through the half-cell reactions

Anodic $Zn(s) \rightarrow Zn^{2+} + 2e^{-}$ [1a]

Cathodic $Cu^{2+} + 2e^{-} \rightarrow Cu(s)$ [1c]

Reports of such electrochemical concepts on cementation reaction appeared in general references[1-3] and also on the copper-zinc cementation reaction in particular work.[4-6] The following observations are noteworthy: (*i*) the reaction is of first order with respect to copper ion concentration and is diffusion controlled. (*ii*) The reaction proceeds through two stages. The slower initial stage corresponds to deposition on a relatively smooth surface and the deposited structure and thickness do not affect the reaction kinetics significantly. The latter stage with an enhanced rate occurs after the deposit reaches some critical thickness (cement critical specific mass) on the surface.

However, recent observations of Zaghib *et al.*[7] suggest the Zn/Zn^{2+} interface parameters and not the cement critical specific mass as the reason for the enhanced rate. The initial concentration of zinc ions, the zinc substrate morphology, and the substrate polarization were also shown as some of the parameters responsible. The present paper aims at an accurate mechanistic conclusion by examining the individual half-cell reactions through polarization measurements.

Experimental

Sample preparation.—Electrolytic grade copper and zinc plates were used as working electrodes with platinum as the counter electrode. After polishing with different grades of emery paper, the exposed surface area (5 cm^2) was degreased with acetone and washed with water before use.

Electrolyte.—The electrolyte constitutes Analar grade $CuSO_4$, K_2SO_4, H_2SO_4, and $ZnSO_4$. The usual composition was 0.0031 M $CuSO_4$ in the presence of 1 M K_2SO_4 at pH 3.5. Variations in specific constituents are mentioned at appropriate places. Unless specified the volume of electrolyte used in each experiment was 100 mL, which was stirred at 120 rpm at ambient temperature (30°C).

Experimental setup.—A two-compartment dual cell as well as a conventional three-electrode cell was used for polarization measurements. In the dual cell, the compartments were separated by a membrane (Cation 61 AZL 389 made by Ionics, Inc., Watertown, MA, USA) to allow the anodic and cathodic half processes to proceed independently. The two electrodes placed in these two compartments (Cu in the cathode chamber and Zn in the anode chamber) were connected externally through a variable resistance and an ammeter. Each electrode was connected to a saturated calomel electrode (SCE) through a voltmeter to record the potential. The potential of each electrode as well as the current in the circuit were recorded by externally decreasing the resistance stepwise from infinitely high value (open circuit) to zero (galvanic contact). A reading was taken at each step after 1 min so that the system attained steady state. The data were used to obtain half-cell polarization curves for the steady-state conditions.

Dynamic current-potential plots at a scan rate of 10 mV/s were also obtained from the conventional three-electrode cell by using model 362 scanning potentiostat of EG&G PAR coupled with series 2000 Omnigraphic X-Y recorder of Houston Instruments Division. The anodic dissolution of a Zn electrode and the cathodic kinetics of a Cu electrode were examined using a platinum counter electrode and an SCE reference electrode, respectively.

Direct cementation reactions were also carried out for comparison with the electrochemical data. These reactions were conducted in a 250 mL vessel containing 100 mL of solution and using a magnetic stirrer. The solution was analyzed from time to time for Cu^{2+} and Zn^{2+} using an atomic absorption spectrophotometer (AAS).

Results

Practical cementation rate.—Figure 1 presents results of copper cementation onto a zinc surface from a sulfate solution of pH 3.5 containing 0.0031 M copper ion at ambient temperature. The stirring rate was 120 rpm, and the exposed zinc surface area was 5 cm^2. Plot 1 in Fig. 1a represents the recorded potential of the electrode against time, which is the mixed potential, E_m, of copper cementation. The plot shows a slight increase in the potential value up to 15 min, which gradually falls back to the initial value. Plot 1 in Fig. 1b presents the deposition of copper against time indicating an initial slow rate up to 10 min. This is followed by a faster rate up to 45-60 min; its current equivalent is 24 mA. Plot 1 in Fig. 1c examines the data for the usual first-order kinetics given by the equation

$$\log([Cu^{2+}]/[Cu^{2+}]_0) = (A_c K_m t)/V = kt \quad [2]$$

where $[Cu^{2+}]$ is the concentration of copper ion at time t, $[Cu^{2+}]_0$ the initial copper concentration, K_m the mass-transfer coefficient of copper ion, A_c the cathodic area, V the volume of solution, and k the kinetic constant. Two stages, one with a slower rate and the other with a higher rate are observed. The results are similar to those observed by the earlier workers.[6,7]

Effect of bath conductivity on polarization.—Polarization studies were conducted in a sulfate solution at pH 3.5 similar to that in the preceding section to examine the half-cell reactions 1a and 1c inde-

S0013-4651(99)04-103-8 CCC: $7.00

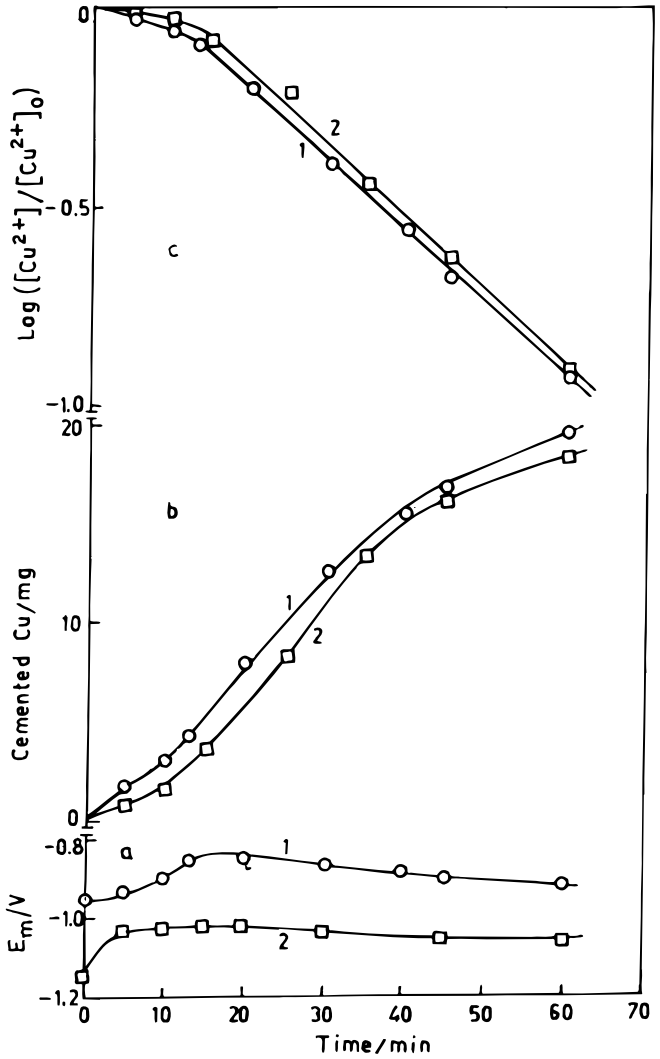

Figure 1. Cementation of copper onto zinc from sulfate solution of pH 3.5 containing 0.0031 M $[Cu^{2+}]$ at ambient temperature. Stirring rate, 120 rpm; exposed zinc surface area, 5 cm^2; (a) mixed potential, E_m, (b) cemented copper in milligrams, and (c) log $([Cu^{2+}]/[Cu^{2+}]_0)$ against time. All plots 2 represent the results in the presence of 1 M K_2SO_4 as supporting electrolyte in the above bath.

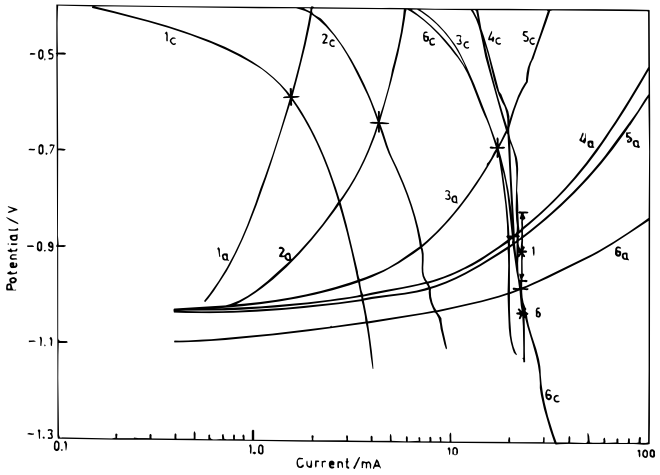

Figure 2. Concurrent polarization plots for copper cementation onto zinc at ambient temperature; pH 3.5; scan rate, 10 mV/s; stirring rate, 120 rpm; exposed zinc surface area, 5 cm^2. a: Anodic plots at different levels of $[Zn^{2+}]$, 1, 0 M; 2, 0.005 M; 3, 0.05 M; 4, 0.42 M; 5, 0.84 M; 6, 0 M + 1 M K_2SO_4. c: Cathodic plots at above different levels of $[Zn^{2+}]$ along with a fixed $[Cu^{2+}]$ of 0.0031 M.

pendently (Fig. 2). Curve 1a in Fig. 2 represents the anodic polarization plot of a zinc electrode in a sulfate solution at pH 3.5. Curve 1c in Fig. 2 in the same figure represents the cathodic polarization of a copper cathode in the same solution along with 0.0031 M copper ion. The resultant mixed potential, (E_m), −0.585 V, and the mixed current, (i_m), 1.6 mA, are obtained from the intersection point. These values differ, to a large extent, from the practical cementation results of −0.900 V and 24 mA (reported in Fig. 1 and also shown in Fig. 2 as *1). This may be due to the poor conductivity of the solution which does not affect the cementation on the same electrode (as in case of Fig. 1) but affects the polarization plots obtained from a circuit with electrodes wide apart. Increase in zinc concentration up to 0.84 M, which improves conductivity, shifts the E_m and i_m closer toward the practical cementation parameters as shown in plots 2-5. To explore the influence of a supporting electrolyte 1 M K_2SO_4 was added to increase the conductivity of the bath (polarization plots 6_a-6_c). Plot *6 shows the practical cementation results in the bath as close to the intersection point of 6_a-6_c plots. Plot 2 in Fig. 1 presents details about deposition under this condition. Though the cementation rate (plot 2 in Fig. 1b) and the first-order plot 2 in Fig. 1c are similar to plots 1, the cementation potential (plot 2 in Fig. 1a) lies below plot 1 resulting from the previous bath. Subsequent experiments were planned with a bath containing 1 M K_2SO_4 to maintain conductivity at reasonable level.

Independent half-cell reactions.—Figure 3 represents two sets of cementation results, one (plot 1) in a bath identical to that presented in plot 2 in Fig. 1, *i.e.*, with 0.0031 M Cu^{2+}, 1 M K_2SO_4, and pH 3.5. In this the zinc dissolution rate (curve b) is higher than the copper cementation rate. Plot 2 in Fig. 3 shows the cementation results in a dual cell setup with zinc electrode in the anode chamber (with no copper ion) and copper electrode in the cathode chamber (0.0031 M copper ion) externally connected for galvanic contact. Both chambers contain 1 M K_2SO_4 at 3.5 pH. Reactions 1a and 1c take place independently in respective chambers due to the potential difference within the galvanic cell. The results show some interesting trends. The anode and cathode potentials (during external contact) differ by around 50 mV, probably due to the ohmic resistance in the circuit. However, these potentials lie above the result from the single bath (plot 1 in Fig. 3a). The copper cementation rate shows only one stage with no enhanced rate (plot 2 in Fig. 3c) thus differing from the practical cementation (plot 1 in Fig. 3c) in a single bath. This implies that the rate is not increased if the electrochemical half-cell reactions of the cementation process are allowed to proceed independently on the zinc anode and the copper cathode. Thus the "cement critical specific mass" does not influence the rate at the Cu^{2+}/Cu interface. Interestingly, the zinc dissolution rate is slightly less than the copper cementation rate (plot 2 in Fig. 3b) indicating that excess zinc dissolution, which may be the result of reaction 3,[8] also does not occur in a dual cell

$$Zn + 2H^+ \rightarrow Zn^{2+} + H_2 \quad [3]$$

$$Zn \rightarrow Zn^{2+} + 2e^- \quad [3a]$$

$$2[H^+ + e^- \rightarrow {}^1/_2H_2] \quad [3c]$$

The enhanced zinc dissolution in the single bath with copper deposition onto the zinc surface (Fig. 3 b1 Zn) might be due to the reaction 3 catalyzed by the deposited copper. This is understandable as the overpotential for the reduction of protons on copper is much less than that of zinc. Also, the pH does not change because the protons removed from the solution by Reaction 3 can be regenerated from the dissociation of bisulfate ions according to reaction

$$HSO_4^- \rightarrow H^+ + SO_4^{2-} \quad [4]$$

Xiong and Ritchie[8] using their experimental data, calculated the p*K*a value to be 1.3 for the reaction and supported this hypothesis. The

S0013-4651(99)04-103-8 CCC: $7.00

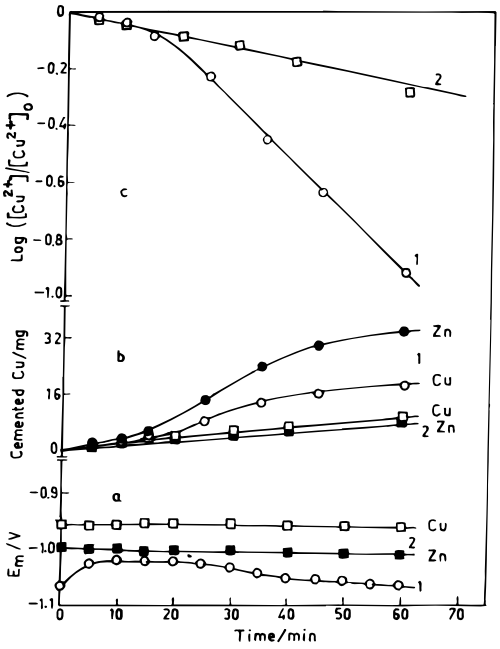

3d
(1),(2),(3)

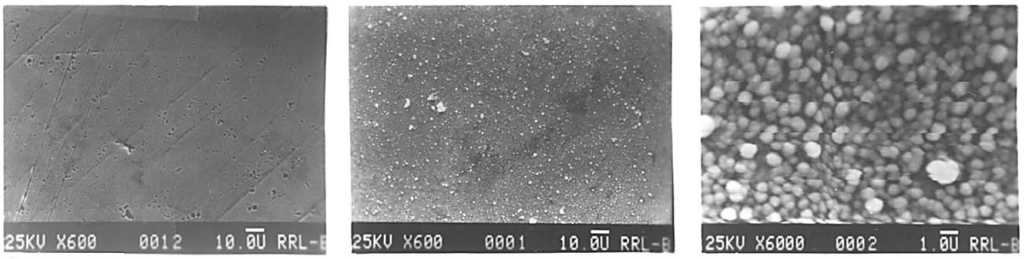

3e
(1),(2),(3)

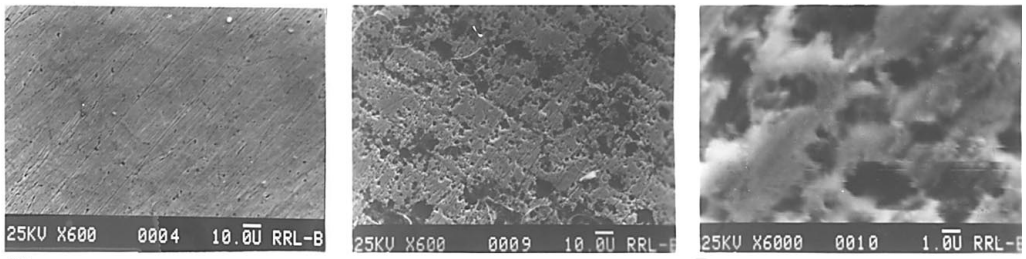

3f
(1),(2)

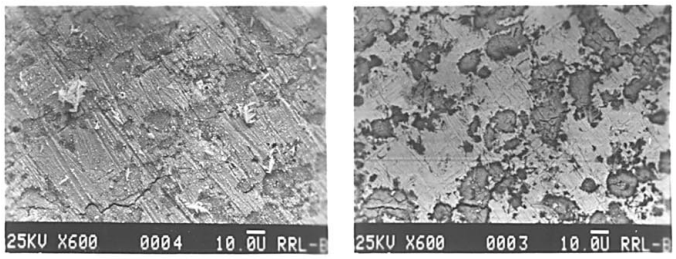

3g
(1),(2),(3)

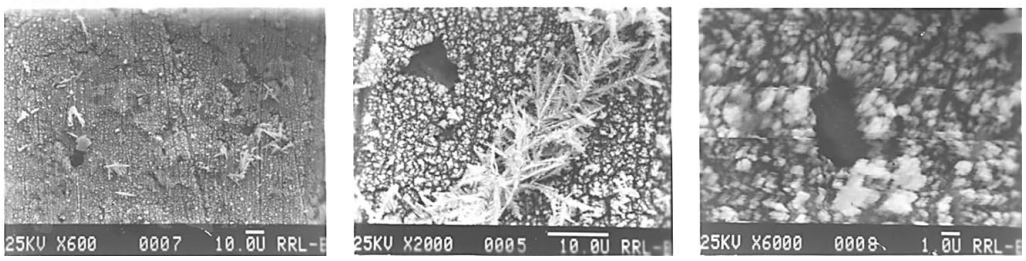

Figure 3. Cementation of copper onto zinc from a sulfate solution of pH 3.5 containing 0.0031 M [Cu^{2+}] and 1 M K_2SO_4 at ambient temperature. Stirring rate, 120 rpm; exposed zinc surface area, 5 cm^2. (a) mixed potential, E_m; (b) cemented copper and dissolved zinc in milligrams; and (c) log([Cu^{2+}]/[Cu^{2+}]$_0$) against time. (All plots 1 represent these conditions.) All plots 2 represent results from dual cell setup with a copper cathode in the cathode chamber and a zinc anode in the anode chamber (no copper ion in the anode chamber). Electrodes are connected externally.
(d) SEM of cemented copper deposition onto zinc metal reflecting copper cathode surface in a two-compartment dual cell where anodic and cathodic reactions occur independently. [Zn^{2+}] 0 M; [Cu^{2+}] 0.0031 M; [K_2SO_4] 1 M; ambient temperature; pH 3.5; stirring rate, 120 rpm. (1) polished Cu (600 times), (2) cemented copper electrode (600 times) exposed for 30 min in the cathode chamber, (3) cemented copper electrode (6000 times) exposed for 30 min in cathode chamber.
(e) SEMs of cemented copper deposition onto zinc metal reflecting anodic zinc surface in a two-compartment dual cell where anodic and cathodic reactions occur independently. [Zn^{2+}] 0 M; [K_2SO_4] 1 M; ambient temperature; pH 3.5; stirring rate, 120 rpm. (1) polished Zn surface (600 times), (2) Zn anode surface (600 times) exposed for 30 min in the anode chamber, (3) Zn anode surface (6000 times) exposed for 30 min in the anode chamber.
(f) SEMs of cemented copper deposition onto zinc metal surface in a single bath. [Zn^{2+}] 0 M; [Cu^{2+}] 0.0031 M; [K_2SO_4] 1 M; ambient temperature; pH 3.5; stirring rate, 120 rpm. (1) 4 min (600 times), (2) 4 min, back scattered (600 times).
(g) SEMs of cemented copper deposition onto zinc metal surface in a single bath. [Zn^{2+}] 0 M; [Cu^{2+}] 0.0031 M; [K_2SO_4] 1 M; ambient temperature; pH 3.5; stirring rate, 120 rpm. (1) 20 min (600 times), (2) 20 min (2000 times), (3) 20 min (6000 times).

S0013-4651(99)04-103-8 CCC: $7.00

present experimental data results in a value of 1.1 for the p*K*a of Reaction 4 and hence a similar conclusion. The value should be close to 2 at infinite dilution.

Morphology.—Figure 3d shows three SEM pictures of copper electrode just before use (no. 1), after 30 min of cementation in the cathode chamber of the dual cell with a magnification of 600 (no. 2) and 6000 (no. 3). The deposit appears smooth. Figure 3e shows three SEM pictures of the surface of zinc electrode dipped in the anode chamber; no. 1 is the freshly polished zinc surface and no. 2 is the surface after 30 min of dipping which shows areas eaten away. No. 3 is the latter surface at a higher magnification of 6000 times. These figures show that change in area due to anodic corrosion (pitting) is significant. However, even this distinct morphology of the anodic and cathodic surfaces did not result in enhancement of rates for either the copper deposition or zinc dissolution. Both no. 1 and 2 in Fig. 3f present the SEM pictures of the zinc surface after 4 min of copper cementation in a 0.0031 M copper bath (initial slower rate region) showing clearcut anodic (pits) and cathodic regions. (g) shows three SEM pictures (at three different magnifications) of the same zinc surface after 20 min of cementation also in a 0.0031 M copper bath. Compared to (f) the anodic pits appear reduced in number as they may have been covered with porous copper deposits. The top layer of the deposit does not appear to be as compact as the one seen in (d).

Polarization measurements.—Figure 4 shows polarization plots for four specific situations. Plots 1_a and 1_c represent the respective anodic (zinc dissolution in the absence of Cu^{2+}) and cathodic (copper deposition on copper) polarization and the intersection point indicates a cementation potential of −0.960 V with a rate (current equivalent) of 23 mA. The practical deposition rate (current equivalent) was 8.12 mA (initial, *1 Cu) and 25.13 mA (enhanced, *1′ Cu). The zinc dissolution rate was 14.58 (*1 Zn) and 45 mA (*1′ Zn). The practical cementation potential was between −1.025 to −1.070 V, which is nearly 0.1 V less than that obtained from the intersection of 1_a-1_c plots. This means that the Zn/Cu^{2+} interaction has a role in decreasing the mixed potential. The plots 2_a-2_c are obtained from the steady-state dual cell experiment and their intersection gives $E_m = -0.945$ V and $i_m = 16$ mA. The deposition of Cu and the dissolution of Zn in this situation were measured to be 8.12 mA (−0.960 V) (*2 Cu) and 6.70 mA (−1.010 V) (*2 Zn), respectively. Plots 3_a-3_c represent polarization curves where only the zinc electrode was used in a bath already containing 0.0031 M copper ion. The starting potential in this case was −1.045 V, which is less than the E_m obtained from 1_a-1_c intersection. The anodic plot 3_a lies below 1_a and indicates a higher dissolution of zinc in the presence of copper. However, plot 3_c merges with 1_c indicating no change in the copper deposition rate on either copper or zinc electrode. Another set of polarization curves 4_a-4_c were plotted in an identical bath using a zinc electrode already cemented for 10 min. The starting potential was −1.075 V, which was less than the E_m obtained from 3_a-3_c plots. Both the anodic (4_a) and cathodic (4_c) curves indicate a higher dissolution rate of zinc and a higher deposition rate of copper in comparison to the 1_a-1_c and 3_a-3_c plots. Thus, the deposited copper enhances the rate for zinc dissolution as well as copper deposition.

Effect of initial electrode treatment.—Figure 5 presents cementation of copper onto zinc electrodes, already treated in different ways. Plot 1 of Fig. 5 is reproduced from plot 1 of Fig. 3. The same zinc electrode, with 25 min of cementation over it, has been dipped in a fresh bath and the results are shown in plot 2. The mixed potential, E_m, is nearly the same as in plot 1 but the deposition starts at a rate corresponding to the second stage and increases further with increase in time (plot 2 in Fig. 5c). Plot 3 corresponds to a zinc electrode in the

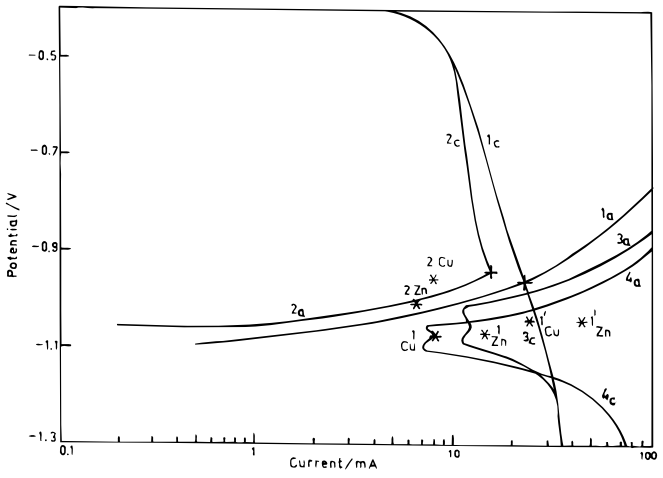

Figure 4. Concurrent polarization curves for copper cementation at ambient temperature; pH 3.5; K_2SO_4, 1 M; scan rate, 10 mV/s (not for plots 2); stirring rate, 120 rpm; electrode surface area, 5 cm^2. a, anodic plots; c, cathodic plots with 0.0031 M $[Cu^{2+}]$. Plots 1, copper cathode, zinc anode individual polarization. 2, zinc anode, copper cathode, simultaneous polarization in a dual cell setup. 3, Fresh zinc electrode in a bath containing 0.0031 M $[Cu^{2+}]$. 4, Zinc electrode with already 10 min cementation in the previous bath (3).

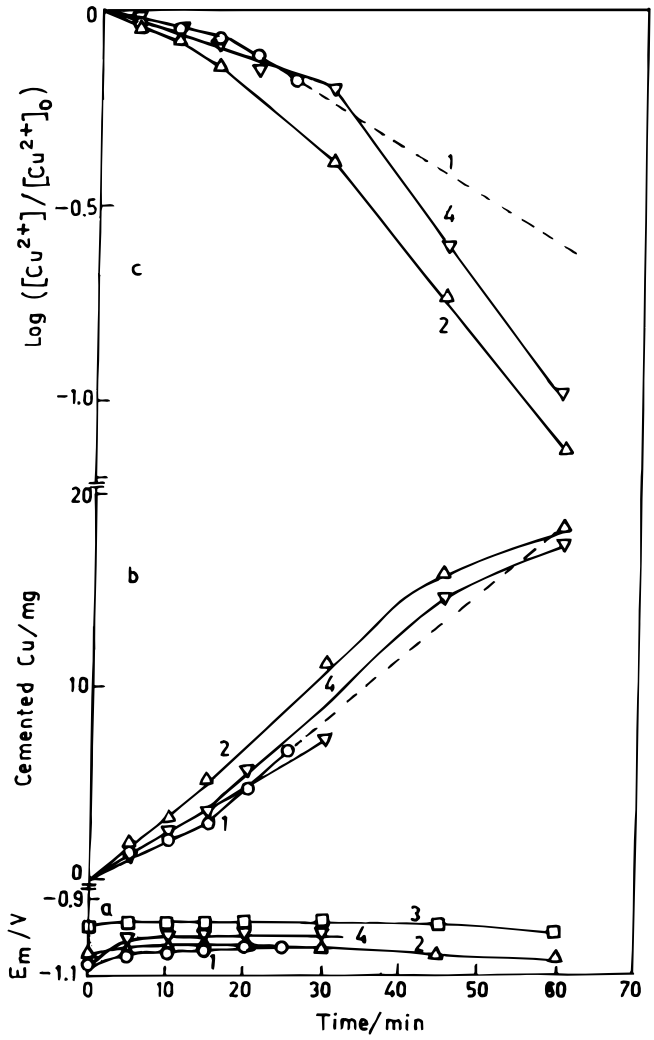

Figure 5. Cementation of copper onto zinc from a sulfate solution of pH 3.5 containing 1 M K_2SO_4, 0.0031 M $[Cu^{2+}]$ at ambient temperature; stirring, 120 rpm; zinc surface area, 5 cm^2. (a) Mixed potential, E_m, (b) cemented copper in milligrams, and (c) $\log([Cu^{2+}]/[Cu^{2+}]_0)$ against time. Plots (1) fresh zinc electrode, (2) zinc electrode with 25 min of cemented copper already on it, (3) zinc electrode in a dual cell, (4) zinc electrode after 60 min of exposure in the anodic chamber of the dual cell.

S0013-4651(99)04-103-8 CCC: $7.00

anode chamber (of dual cell) which presents only the potential (3 in Fig. 5a) and no copper deposition. After being exposed in the dual cell the zinc electrode was dipped in a fresh bath for copper cementation, and the results are shown in plot 4. The potential (4 in Fig. 5a) is slightly more than that in plots 1 and 2. The initial rate (4 in Fig. 5b and c) is faster than the initial rate with a fresh electrode (1 in Fig. 5b and c) which is probably due to the availability of more exposed surface area due to pitting. The shift toward a higher rate is delayed when compared to the fresh electrode. This enhanced rate corresponds to that of the copper-cemented electrode (2 and 4 in Fig. 5b and c) and implies that prior polarization of the zinc electrode also has a role in the enhancement of the cementation rate.[7] However, the initial rate shown by plot 2 is higher than the enhanced rate of plot 1 and the initial rate of plot 4, indicating the role of deposited copper also. Hence, the significance of the anodic surface as well as deposited copper in copper cementation.

Effect of extra galvanic contact.—One of the important observations in the above mentioned experimental results is the decrease in the mixed potential, E_m, when zinc is immersed in the solution containing copper ion. This is in comparison to the E_m observed in the dual cell experiment. This shift increases when cemented copper is already present on the zinc surface although the potential of a copper electrode is much higher. Earlier workers[7,9] have indicated the effect of constant impressed polarization on copper cementation. For further insight into this aspect, two cementation experiments were conducted in the dual cell setup with one chamber having a zinc electrode (called a working electrode) in a copper-containing bath (0.0031 M Cu^{2+}, 1 M K_2SO_4, 3.5 pH) similar to the single bath. In one case (the first experiment), the second chamber was maintained with an identical bath having a copper electrode externally connected to the working zinc electrode. The aim was to shift part of the cathodic reaction to the second chamber via current flow through the external galvanic contact. This resulted in an average flow of only 2.0 mA (9.3 to 1.3 mA) current with a deposition of about 2.5 mg copper in 60 min on the copper electrode in the other chamber. In the next experiment, the second chamber contained another zinc electrode immersed in a bath devoid of copper ion and connected externally to the working zinc electrode. Here a portion of the anodic process is shifted to the second chamber imposing a flow of current through extra galvanic contact. A flow of around 0.4 mA (0.15 to 0.64 mA) current resulted with the dissolution of 0.4 mg zinc in 60 min from the zinc electrode in the other chamber. The results of the working zinc electrode for both the experiments are presented in Fig. 6. Plot 2 refers to the first experiment and plot 3 to the second experiment. Plot 1 obtained for a zinc electrode in the absence of extra galvanic contact (same as Fig. 1, plot 2), is given for comparison. Plot 2 in Fig. 6a indicates a slight increase in the mixed potential, E_m, in comparison to E_m of plot 1 while there is a decrease in

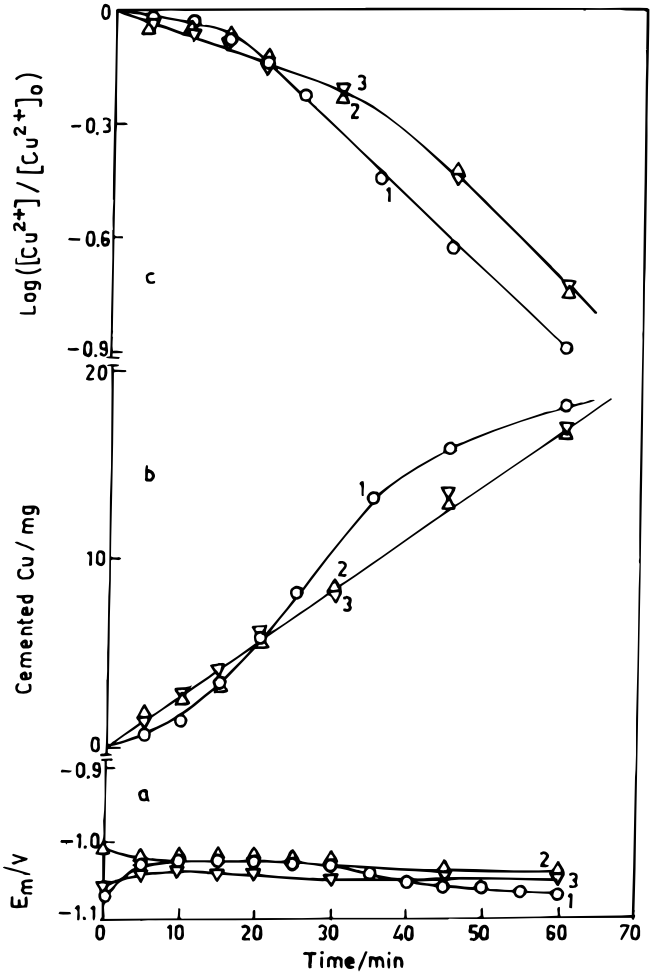

Figure 6. Cementation of copper onto zinc from a sulfate solution of pH 3.5 containing 1 M K_2SO_4, 0.0031 M [Cu^{2+}], at ambient temperature; stirring rate, 120 rpm; exposed zinc surface area, 5 cm^2. (a) Mixed potential, E_m, (b) cemented Cu in milligrams, and (c) log([Cu^{2+}]/[Cu^{2+}]$_0$) against time, (1) zinc electrode, (2) zinc electrode in one chamber of a dual cell connected externally to the copper electrode in the other chamber, (3) zinc electrode in one chamber of a dual cell connected externally to the zinc electrode in the other chamber (in absence of Cu^{2+} ion).

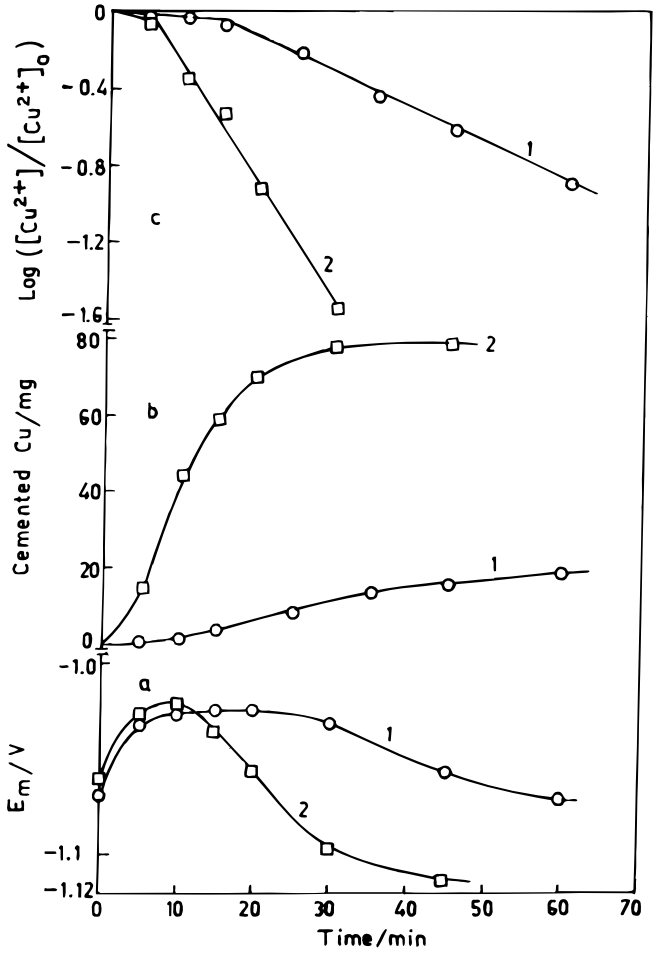

Figure 7. Cementation of copper onto zinc from a sulfate solutions at 2 levels of [Cu^{2+}] in the bath, (1) 0.0031 M, (2) 0.0126 M, pH 3.5, K_2SO_4: 1 M, ambient temperature, stirring rate, 120 rpm; exposed zinc surface area, 5 cm^2. (a) Mixed potential, E_m, (b) cemented copper in milligrams, (c) log([Cu^{2+}]/[Cu^{2+}]$_o$) against time.

S0013-4651(99)04-103-8 CCC: $7.00 © The Electrochemical Society, Inc.

E_m in the case of plot 3. Plots 2 and 3 in Fig. 6b indicates a similar deposition rate and the S shape of 1 seems to have been smoothened. Plots 2 and 3 in Fig. 6c are close to each other with a higher initial rate compared to the initial rate of plot 1. The enhanced rate of plots 2 and 3 is close to that of 1 though appearing at a later time. The anticipated shift of the cathodic and anodic reactions, respectively, in the first and second experiments was only partial and the dissolution of zinc and deposition of copper on the working zinc electrode were continuous. Zinc dissolution (27 mg equivalent of copper) after 60 min in each case, is greater than the 16 mg of the copper cementated during this time. The rise in the initial rate may be due to the extra galvanic contact. The shift in time for the enhanced rate is probably due to the partial shift of one of the half-reactions into the other chamber. Thus interaction of Zn/Cu^{2+} plays an important role in the entire process.

Effect of bath composition.—Experiments have also been carried out to study the effect of bath composition on the cementation of copper onto zinc. Figure 7 presents such cementation results at copper concentrations of 0.0031 and 0.0126 M. The cementation rate increases remarkably with the increase in copper ion concentration. Figure 8 shows the concurrent polarization plots for copper cementation onto zinc at five levels of copper concentration. In Fig. 9 the mixed potential, E_m, and the mixed current, i_m, obtained from Fig. 8 were plotted against the copper concentration. The E_m gives a slope of 0.105 V per decade and log i_m gives a slope of 0.43. Current values obtained at cathodic overpotentials of −0.8 and −0.6 V were also plotted in Fig. 9a (plots 2 and 3) resulting in slopes of 0.54 and 0.76, respectively; a slope of 1 is expected if the cementation rate is controlled by diffusion of copper ions. However, the rate constant k obtained from practical deposition data of Fig. 7c gives values closer to 1, *i.e.*, 1.08 from the initial rate (plot 4 in Fig. 9a) and 0.86 from the enhanced rate (plot 5 in Fig. 9a) indicating that the cementation process is controlled by diffusion. The discrepancy in the polarization data may be attributed to Reaction 3, which takes place simultaneously. This is dealt with in detail in a later section.

Figure 10 presents the cementation results obtained with 0.1 M zinc ion in the bath. Compared to the values obtained with no zinc in the bath (plot 1 in Fig. 10), the deposition potential is slightly higher in the beginning but is lower after 5 to 30 min. However, the rate of copper cementation did not differ appreciably with a change in bath conditions; only the onset of the enhanced rate stage was delayed. That the rate was rather low during the second stage has been reported by earlier workers also.[7,9] The polarization plots (not shown here) also do not vary significantly, in E_m and i_m, with zinc concentration in the bath.

Protonation reaction.—It was mentioned above that excess zinc dissolution via Reaction 3 is also possible during the cementation of copper onto zinc. Hence the need to study the effect of pH. Polarization experiments were conducted at pH values of 3.5, 2.5, 1.5, and 0.76 and the resulting mixed potential, E_m and the mixed current, i_m, were plotted against log $[H^+]$ as shown in plot 1 in Fig. 11. The E_m gives a slope of 0.057 V per decade (plot 1 in Fig. 11b) and the i_m gives a slope of 0.25 (plot 1 in Fig. 11a). Figure 12 presents the practical cementation results at pH values of 3.5 (1) and 1.5 (2). The cementation rate of copper does not show any significant change with change in pH. Therefore, the effect of pH on E_m and i_m, shown in Fig. 11, is probably due to Reaction 3. It has also been observed (Fig. 3) that excess zinc dissolves, if copper is cemented onto the zinc electrode. Plots of this excess dissolved zinc, in terms of milligram equivalent of copper *vs*. time at (1) 3.5 pH and 0.0031 M copper ion, (2) 1.5 pH and, 0.0031 M copper ion, and (3) 3.5 pH and 0.0126 M of copper ion are presented in Fig. 13a. These plots clearly indicate that excess zinc dissolution increases with an increase in $[H^+]$ as well as $[Cu^{2+}]$. These rates were converted into current equivalents by applying Faraday's law, and the data at two pH values is presented in plot 2 in Fig. 11a. The resulting slope is 0.5 and is expected when E_m lies on the Tafel portions of the individual halves of Reaction 3. Plot 1 gives a low value because of the simul-

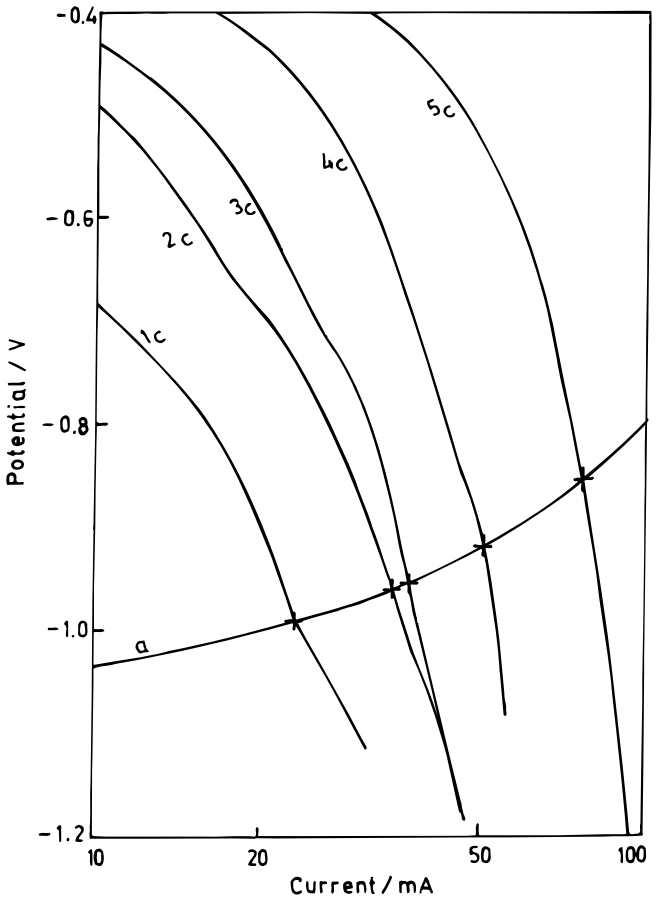

Figure 8. Concurrent polarization plots for copper cementation onto zinc at ambient temperature, pH 3.5; $[K_2SO_4]$: 1 M; scan rate, 10 mV/s; stirring rate: 120 rpm, electrode surface area, 5 cm^2; a, anodic; c, cathodic; (1) 0.0008 M, (2) 0.0016 M, (3) 0.0031 M. (4) 0.0062 M, (5) 0.0124 M $[Cu^{2+}]$.

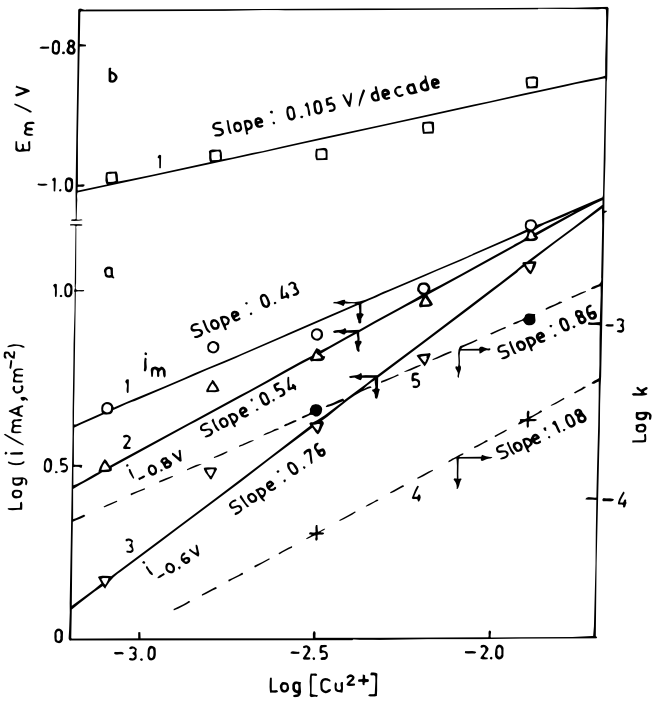

Figure 9. (a) Log i_m, log k, and (b) E_m *vs*. log $[Cu^{2+}]$ plots.

S0013-4651(99)04-103-8 CCC: $7.00

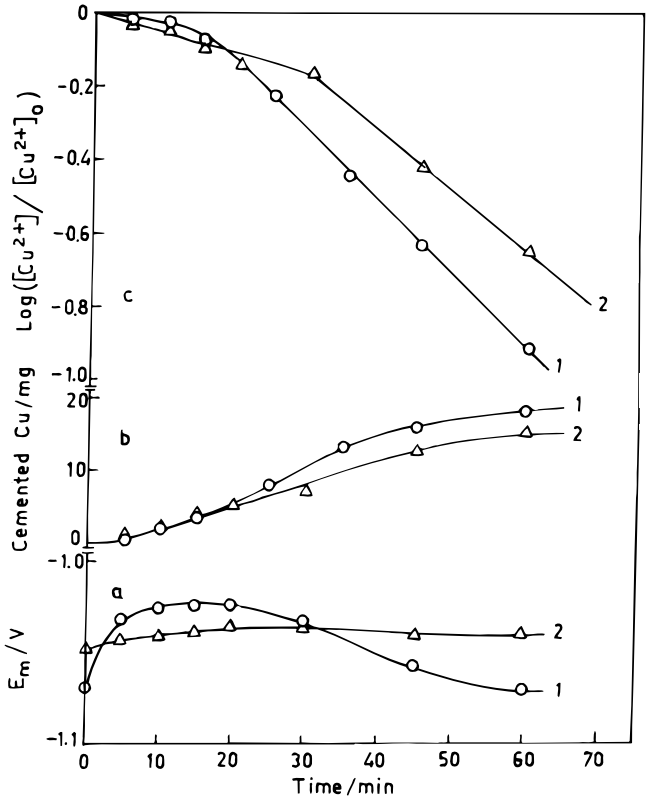

Figure 10. Cementation of copper onto zinc from a sulfate solution of pH 3.5 containing 1 M K_2SO_4, 0.0031 M [Cu^{2+}] along with (1) 0 M [Zn^{2+}], and (2) 0.1 M [Zn^{2+}] and at ambient temperature; stirring rate, 120 rpm; exposed zinc surface area, 5 cm^2. (a) The mixed potential, E_m; (b) copper cemented in milligrams, and (c) log([Cu^{2+}]/[Cu^{2+}]$_0$) *vs.* time.

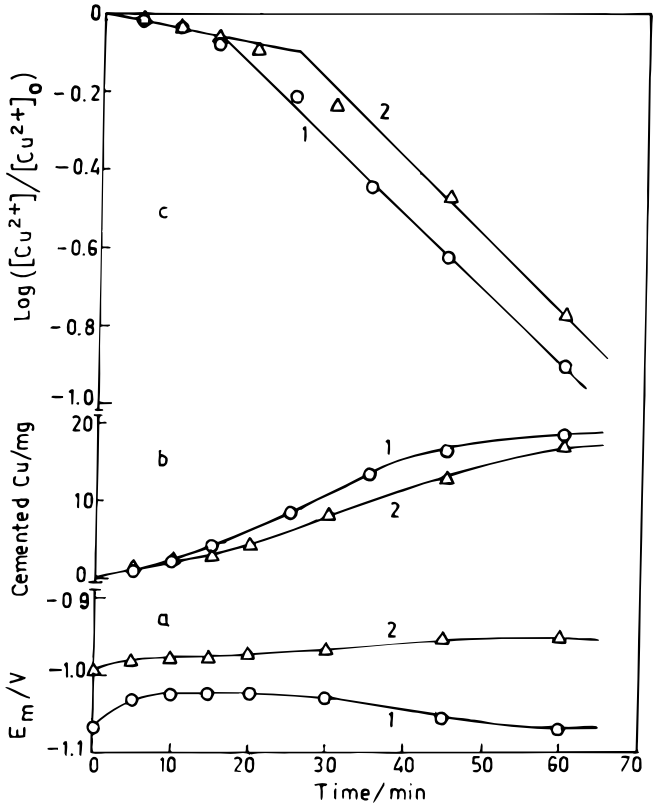

Figure 12. Cementation of copper onto zinc at two levels of pH (1) 3.5 and (2) 1.5 in a bath containing 1 M K_2SO_4 and 0.0031 M [Cu^{2+}] at 120 rpm stirring; exposed zinc surface area, 5 cm^2. (a) Mixed potential E_m, (b) copper cemented, and (c) log([Cu^{2+}]/[Cu^{2+}]$_0$) *vs.* time.

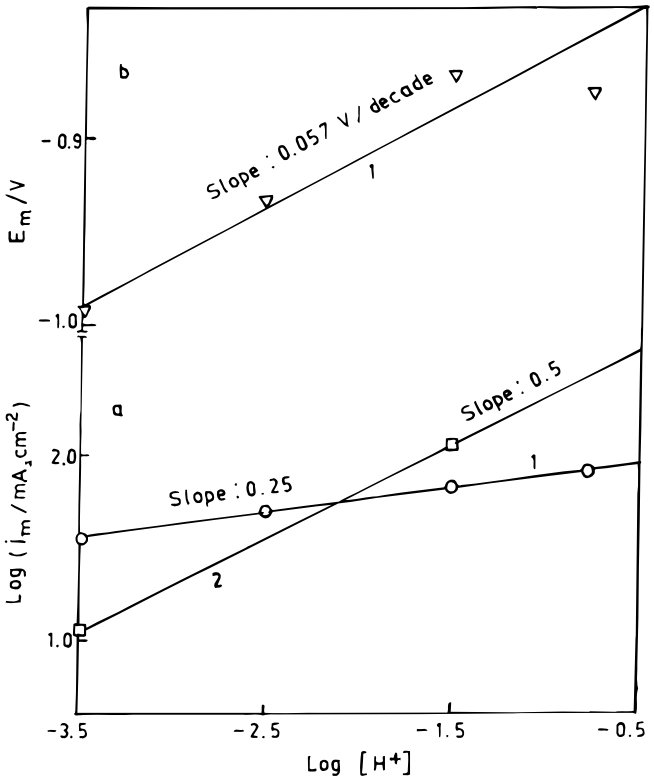

Figure 11. (a) Log i_m and (b) E_m *vs.* log [H^+] plots for copper cementation onto zinc. (1) Data obtained from polarization plots, (2) data obtained from zinc dissolution.

taneous copper cementation reaction which is not affected by pH. Intersection of these plots at pH 2.1 indicates that at pH below this value Reaction 3 is significantly high. Excess zinc dissolution is as high as 0.0375 mg copper equivalent(s) (113.1 mA) at pH 1.5 compared to 0.0036 mg copper equivalent(s) (10.86 mA) at pH 3.5. The copper cementation rate, however, is nearly constant at both of these pH levels. That the excess zinc dissolution rate increases with an increase in copper in the bath supports the view that Reaction 3 occurs only when it is catalyzed by copper. This is further supported by the absence of excess dissolution in the absence of copper in the anode chamber of the dual cell. The presence of 0.0126 M copper ion in the bath resulted in an excess zinc dissolution rate of 0.0098 mg copper equivalent(s) (29.56 mA) (plot 3 in Fig. 13a) as against 0.0036 mg copper equivalent(s) (10.86 mA) (plot 1 in Fig. 13a) at 0.0031 M copper ion in the bath. The morphology of the electrode surface at 0.0126 M copper in the bath is interesting. The deposit, particularly the outermost region, appears very bulky, porous, loosely attached, and can be easily removed even by rinsing lightly with water. Figures 13b and c show SEM pictures at two magnifications of this surface after removal of the top layer. The porous morphology clearly appeared although the innermost cemented copper layer was strongly adherent to the zinc surface. The cemented copper prevents a clear assessment of the morphology of the inner zinc surface, despite the extensive quantity of *ca*. 35 mg of zinc dissolution.

Discussion

Kinetic equation for cementation.—The cementation Reaction 1 proceeds through the half-cell Reactions 1a and 1c along with excess zinc dissolution due to Reactions 3a and 3c. As Reactions 1a-1c and 3a-3c follow the electrochemical principles, kinetic equations can be developed in a straightforward manner. Apparently Reaction 1 takes place in the Tafel region of 1a and limiting current region of 1c while Reaction 3 occurs in the Tafel region of both 3a and 3c. In fact Reac-

S0013-4651(99)04-103-8 CCC: $7.00

tions 1a and 3a are the same and the current-potential relationship for the Tafel portion of this anodic reaction may be expressed according to the Butler-Volmer equation

$$i_a = n_a A_a k_a F \exp\{n_a^{rds} \beta F E_a / RT\} \quad [5]$$

Here i, k, n_a, A, F, n_a^{rds}, β, E, R, and T are the current density, rate constant, number of electrons participating in the reaction, electrode area, Faraday's number, number of electrons participating in the rate-controlling step, transfer coefficient, electrode potential, universal gas constant, and absolute temperature, respectively. The subscripts a and c refer to anode and cathode reactions, respectively. The cathodic partial equation 1c is described by Nernst equation as follows

$$-i_c = F A_c n_c D_c [Cu^{2+}]/d_c \quad [6]$$

Here D and d denote the diffusivity of the diffusing species and the thickness of the diffusion layer, respectively. At the mixed potential E_m, $i_a = -i_c$. Equating Eq. 5 and 6 and assuming that, $n_a^{rds} = n_c^{rds} = 1$, $n_a = n_c = 2$, and $\beta_a = \beta_c = 1/2$ gives the following expression for E_m

$$E_m = \{(4.606RT)/F\} \log\{(A_c D_c [Cu^{2+}])/(k_{af} A_a d_c)\} \quad [7]$$

At this condition $i_m = i_a = -i_c =$ Eq. 6.

Equations 6 and 7 indicate that E_m results in a dependence of $(4.606RT)/F$ or 0.118 V per decade of $[Cu^{2+}]$ at 298 K, and i_m gives a slope of 1 in this condition. $[H^+]$ may not have any direct effect on this reaction. However, deposited copper has a catalytic effect on Reaction 3, and the polarization plots obtained would represent a combination of Reactions 1 and 3. Therefore, the effect of $[H^+]$ must be considered when polarization data are to be generalized.

Kinetic equation for protonation reaction.—In a similar way kinetic equation for E_m and i_m can be generated for Reactions 3a and 3c. Applying the Butler-Volmer equation to Reaction 3c, a current-potential relation can be given as

$$-i_c = n_c A_c F k_{cf} [H^+] \exp\{-n_c^{rds}(1 - \beta_c) F E_c / RT\} \quad [8]$$

The expression for E_m and i_m are

$$E_m = \{(2.303\ RT)/F\} \log\{(A_c k_{cf}/2A_a k_{af})\ [H^+]\} \quad [9]$$

$$i_m = F(n_a A_a k_a n_c A_c k_c\ [H^+])^{1/2} \quad [10]$$

These two equations imply that the E_m will have a dependency of 0.059 V per decade of $[H^+]$ at 298 K and log i_m will have a slope of 0.5 on log $[H^+]$. Figures 9 and 11 reveal that the values derived from the polarization plots are equivalent to a combination of the two reaction schemes. For example, 0.105 V per decade (Fig. 9) is in between 0.059 (Eq. 9) and 0.118 V (Eq. 7), 0.25 (Fig. 11) is in between 0, dependency of i_m of Reaction 1 on $[H^+]$ (Eq. 6) and 0.5, dependency of i_m of Reaction 3 on $[H^+]$ (Eq. 10). However, the kinetic rate constant (in Eq. 2), measured independent of copper cementation and excess zinc dissolution, provides the exact dependency of Reaction 1 for copper cementation rate on $[Cu^{2+}]$ (Fig. 9) for both the initial (1.08) and enhanced rates (0.86); k is 0.5 for dependency of excess zinc dissolution on $[H^+]$ (Fig. 11).

Rate enhancement.—The copper deposit on the copper electrode in the dual cell cathode chamber is smooth and its morphology does not play a role. However, in a practical cementation process both polarization of Zn/Zn^{2+} half-reaction and morphology of cemented copper, do play a role. The E_m which is closer to E_a initially increases during the first 10-15 min, remains constant for sometime, and then decreases. The E_m observed from the polarization curve is far from the cathodic rest potential and is closer to the anodic rest potential. This indicates that the rate of the cementation process is controlled by the cathodic half-reaction, Cu^{2+}/Cu, which is slower than the anodic half-cell, Zn/Zn^{2+}. It is, therefore, natural that the initial E_m during practical cementation is toward the dominant anodic Zn/Zn^{2+} cell. After stabilization it remains constant for sometime and then slowly decreases due to a decrease in copper ion concentration as cementation proceeds.

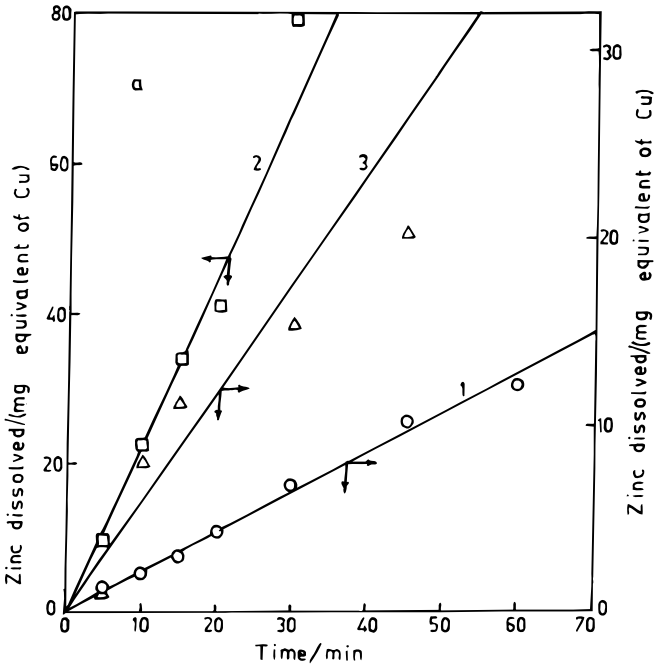

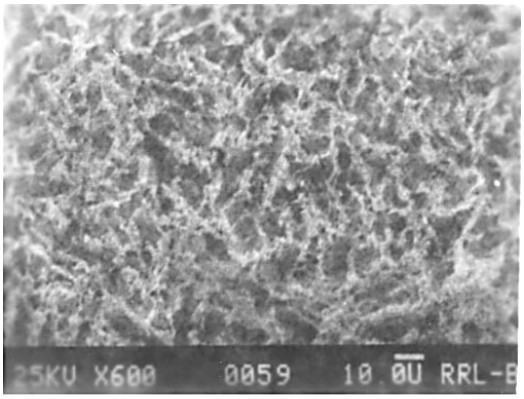

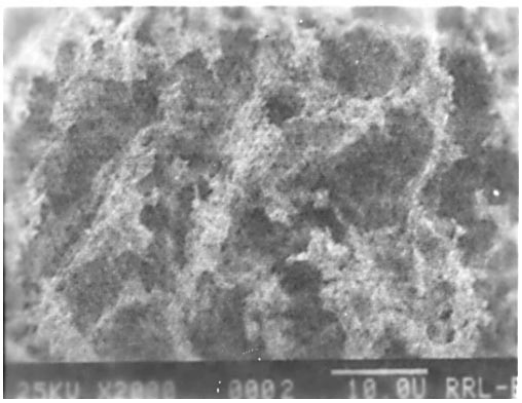

Figure 13. (a) Excess zinc dissolution (in terms of milligram equivalent of copper) during cementation of copper onto zinc in presence of 1 M K_2SO_4. Stirring rate, 120 rpm; exposed zinc surface area; 5 cm^2 plots (1) $[Cu^{2+}]$ 0.0031 M; pH 3.5; (2) $[Cu^{2+}]$ 0.0031 M, pH 1.5; (3) $[Cu^{2+}]$ 0.0126 M, pH 3.5. (b) SEMs of cemented copper deposition onto zinc metal surface in a single bath. $[Zn^{2+}]$ 0 M, $[Cu^{2+}]$ 0.0126 M, $[K_2SO_4]$ 1 M, ambient temperature, pH 3.5, stirring rate; 120 rpm. (1) 20 min (600 times), (2) 20 min (2000 times).

S0013-4651(99)04-103-8 CCC: $7.00

It can be visualized that the two cells, *i.e.*, (*i*) Zn/Zn^{2+}-Cu^{2+}/Cu and (*ii*) Zn/Zn^{2+}-H^+/H are in operation simultaneously with the Zn/Zn^{2+} as common, possibly with the same common anodic area. The cathodic site for H^+/H half-cell is probably the surface of the deposited copper. Since the deposited copper has a catalytic role in Reaction 3, its morphology (surface area) becomes important. Plot 2 in Fig. 13a also indicates enhancement in excess zinc dissolution after 20 min. The surface area of the anodically polarized zinc electrode also increases because of zinc dissolution, though not to the extent of the increase in the deposited copper area. The enhanced rate, therefore, can be the result of the enhanced area of both the anodic and cathodic sites. It may also be noted that the rate of a cathodic reduction process with its half-reaction under limiting current region (Fig. 2 and 4) can be increased only when its cathodic area or concentration of the diffusing species is increased and the cathodic plot shifts to higher values in the current axis. Any change in the anodic plot alone does not increase i_m (the Cu cementation rate) when the cathodic half is in the limiting current region. Accordingly, the presence of a zinc electrode with deposited copper on it provides (*i*) a copper deposit with morphology different from that of the copper substrate, (*ii*) a copper deposit capable of catalyzing hydrogen reduction, and (*iii*) a zinc surface with changed morphology due to corrosion of its anodic surface. These factors probably play a role in the rate enhancement process of copper cementation with the first two shifting the E_m in the current scale toward higher i_m while the last one shifts the E_m toward lower values.

A point may be made regarding the effect of the externally connected half-cell on the zinc working electrode being cemented in a bath as in Fig. 6. Only part of the cathodic or anodic half-cell of the Zn/Zn^{2+}-Cu^{2+}/Cu cell shifts away from the working zinc electrode while a major part of the reaction takes place on the working zinc electrode itself as the resistance between sites within a single electrode is less than between two electrodes separated by a distance through a circuit. In the case of the externally connected zinc electrode the Zn/Zn^{2+}-H^+/H couple do not shift because the reaction does not take place on a zinc electrode without deposited copper on it as catalyzing agent. Consequently the anodic half-cell of Zn/Zn^{2+}-Cu^{2+}/Cu couple gets shifted partially to improve the cathodic site on the working electrode increasing the initial rate of deposition. In the case of an externally connected copper electrode, an extra driving force was imposed by shifting the (E_m, i_m) toward higher values and hence the initial increased rate (Fig. 6, plot 2 rise in an initial E_m value and an initial rate). The reason for the enhancement remains the same, *i.e.*, increase in surface area due to morphology of the deposited copper and dissolved zinc.

Diffusion layer thickness.—It is also possible to assess the diffusion layer thickness from the experimental *k* value. Equation 2 may be rewritten as follows[1]

$$\log([Cu^{2+}]/[Cu^{2+}]_0) = (fAD)t/(2.303\ Vd_c) \qquad [11]$$

Here, *A* is the geometric area of the sample and *f* is the ratio of the true cathodic area to the geometric area, or $f = A_c/A$. Wadsworth[1] has suggested the *D* values of typical cementation solution concentrations to be about 0.5 to 2×10^{-5} cm^2 $(s)^{-1}$ at 25°C and that of 0.02 M Cu^{2+} to be 0.67×10^{-5} cm^2 $(s)^{-1}$. Assuming $A_c = A_a$, *f* can be taken as 0.5 in the initial stage of concentration. A d_c value of 1.5×10^{-3} cm was obtained using a typical initial *k* value of this study along with the above mentioned *D* value of Cu^{2+}. During the enhanced rate of cementation, *f* may be higher and may range from 0.5 to 3 as indicated by Wadsworth.[1] Taking the enhanced rate of a typical result from this study a d_c value of 2.7×10^{-4} to 1.6×10^{-3} cm may be calculated. The latter value is close to the d_c value of 1.5×10^{-3} calculated above from the initial *k* value with $f = 0.5$. This indicates the rise in deposit surface area as the reason for rate enhancement. The d_c values are also comparable to those reported in the literature.[1]

Conclusions

From this study the following conclusions may be made.

1. Cementation of copper onto a zinc substrate from a sulfate solution follows a first-order process with respect to $[Cu^{2+}]$. The initial rate is followed by a second stage with an enhanced rate. Zinc dissolution via hydrogen reduction also takes place simultaneously.

2. Isolation of the anodic (Zn/Zn^{2+}) and cathodic (Cu^{2+}/Cu) half-cell reactions into independent anodic and cathodic chambers of a dual cell results in only the first stage of dissolution behavior and proton reduction does not exert a significant effect.

3. Hydrogen reduction reaction is catalyzed by the deposited copper on a zinc surface. The protons removed from the solution might be regenerated by the dissociation of bisulfate ions.

4. The second step of the enhanced rate is associated with a decrease in E_m values and an increase in both anodic and cathodic surface sites on the zinc electrode.

5. Polarization measurements substantiate these results and indicate that a transport-limited cathodic reduction of Cu^{2+} to Cu controls the process.

6. Expressions for E_m and i_m were derived for copper cementation based on electrochemical principles. Similar expressions were also derived for zinc dissolution via hydrogen reduction. Results obtained from the experiments fit well into the derived expressions.

Acknowledgments

The authors thank Professor H. S. Ray, Director, and Dr. R. P. Das, Scientist-G and Head, Hydro and Electrometallurgy Division, Regional Research Laboratory, Bhubaneswar, for their encouragement during the study and their kind permission to publish this paper. They also thank Dr. J. R. Rao, Deputy Director, Regional Research Laboratory, Bhubaneswar, for his help during the preparation of the manuscript.

References

1. M. E. Wadsworth, *Trans. Met. Soc., AIME*, **245**, 1381 (1969).
2. J. D. Miller, in *Rate Process in Extractive Metallurgy*, H. Y. Sohn and M. E. Wadsworth, Editors, p. 197, Plenum Press, New York (1979).
3. G. P. Power and I. M. Ritchie, in *Modern Aspects of Electrochemistry*, Vol. 11, B. E. Conway and J. O'M. Bockris, Editors, p. 199, Prentice Hall, Englewood Cliffs, NJ (1975).
4. C. V. King and M. M. Burge, *J. Electrochem. Soc*., **65**, 403 (1934).
5. M. Centnerswer and W. Heller, *Z. Physik, Chem*., **Abt. A**, 113 (1932).
6. P. H. Strickland and F. L. Lawson, *Proc. Aust. Inst. Min. Met*., **236**, 225 (1970).
7. K. Zaghib, E. Chainet, and B. Nguyen, *J. Electrochem. Soc*., **144**, 3772 (1997).
8. J. Xiong and I. M. Ritchie, *Hydrometallurgy*, **16**, 301 (1986).
9. K. Zaghib, E. Chainet, and B. Nguyen, *Electrochim. Acta*, **35**, 657 (1990).